Chapter 5

Interplay of disorder and amplification in a passive medium with active scatterers : Monte Carlo simulation

5.1 Motivation

In chapter 1, we had discussed the basic types of RAMs that have been studied, so far, and had classified them into two types, namely

(1) *The dye-scatterer RAM or the Direct-RAM (D-RAM)*, which consists of amplifying bulk medium (continuum) containing small (discrete) scatterers. Here, the continuum medium is active while the discrete scatterers are passive, e.g., an optically pumped laser dye solution (Rhodamine 6G in ethanol; continuum medium), with a suspension of TiO_2 or polystyrene microspheres (passive scatterers).

(2) *The crushed laser crystal or the Reverse-RAM (R-RAM)*: Here, in contrast to the D-RAM, it is the scatterers which are active while the continuum medium is passive, e.g., the fluorescent polystyrene microspheres suspended in a passive medium like ethanol, or semiconductor Zinc Oxide (ZnO) or Gallium nitride (GaN) powder microspheres. It can also be realized as crushed laser crystals (e.g. ruby or Ti:Sapphire). These later systems are highly concentrated and a clean spatial separation of the gain medium and the scattering

does not exist. These cases are best viewed as a medium with randomly varying real and imaginary parts of the refractive index.

The work presented in this chapter is motivated by the interesting possibility, at least in principle, arising out of the reversal of roles of the scatterers and the medium. Thus, in a D-RAM the propagation medium is active (amplifying) but does not scatter, while the scatterers are passive and therefore do not amplify. In contrast to this, in an R-RAM the medium is passive and propagates the photon without amplification, while the scatterers are active and amplify even as they scatter the photons. More specifically, in a D-RAM light amplification occurs in the active bulk *during* transit between two successive scattering events giving an exponential gain factor $exp(L/l_g)$, where L is the total path length traversed by the photon in the active medium before finally exiting it, and l_g the gain length. The enhancement of the total path length traversed by the multiply scattered photon diffusing through the active medium leads to the enhanced gain, and hence possibly to lasing through the distributed positive feedback. In such a D-RAM, the gain increases monotonically with increase in the scattering strength (via increased scatterer size (d), scatterer density (n_s) or the refractive index mismatch (δn) between the passive scatterers and the active bulk). In an R-RAM, on the other hand, there is no amplification in-between two successive scattering events (the continuous medium being passive). Instead, the amplification takes place only within the active scatterers, i.e., when the light encounters and penetrates the active scatterers (Fig. 5.1). It is thus clear that the various factors like the scatterer size (d), scatterer density (n_s), refractive index mismatch (δn) between the bulk (continuum) and the scatterers (discrete), and the gain (l_g^{-1}) will affect the emission intensity qualitatively differently in the two types of RAMs. In fact, in an R-RAM we expect to observe an interesting competition between multiple scattering (controlled by the refractive index mismatch) and the gain inherent in the active scatterers – while the higher refractive index mismatch between the active scatterers and the passive medium gives the expected enhanced diffusive path length (normally conducive to enhanced gain as indeed observed in a conventional D-RAM), the very same high refractive index mismatch can also give a reduced penetration of the photon into the interior of the active scatterers, thus tending to diminish the overall intensity gain. This competition

may lead to a non-monotonic dependence of the overall gain on the refractive index mismatch for a suitable range of the parameter values characterizing the R-RAM. Ultimately, the competition is between the effectiveness of the individual amplifying scattering events and how frequent are these multiple scattering events. This interplay of disorder (multiple scattering) and amplification provides the main motivation for our present study which is a Monte Carlo simulation of the photon diffusion in an optically pumped R-RAM. The main findings of our simulation are, (1) a monotonic decrease in the overall gain with the increase in mismatch in the limit of small gain length (opposite to that observed in D-RAMs), (2) a monotonic rise in the overall gain with increase in the refractive mismatch (scattering) for large gain length, and (3) a non-monotonic dependence of the overall gain on the refractive index mismatch for intermediate values of the gain length.

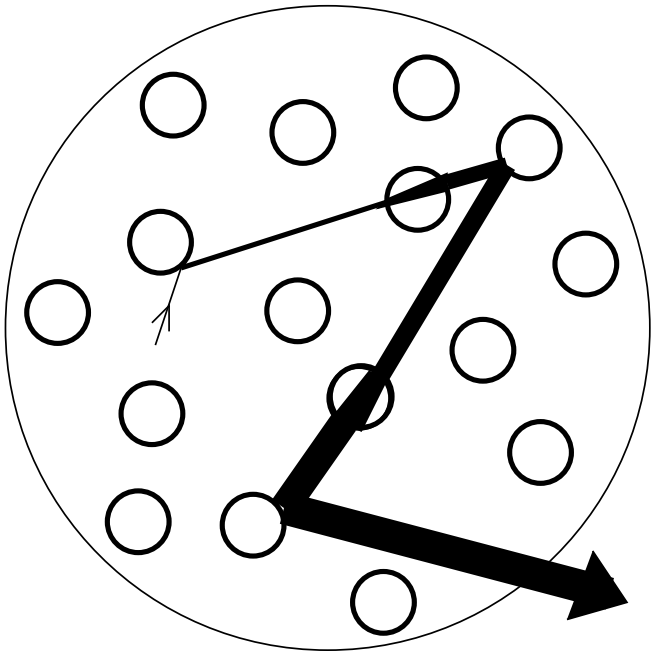

Figure 5.1: *Schematic of a crushed laser crystal RAM (with active scatterers embedded in passive bulk). Line thickness is indicative of intensity.*

It is apt to point out here that an analogous competition should be observable, in principle, in the usual context of extinction due to lossy scatterers – here again, a higher refractive index mismatch would give higher cross-section (σ_s) of photon scattering out of the incident

direction, but at the same time give a lower absorption cross-section (σ_a) because of the lesser penetration of the photon into the lossy interior of the scatterers. This will make the net scattered intensity a non-monotonic function of the refractive index mismatch in general.

Before we present our Monte Carlo simulations of photon diffusion in an R-RAM, we turn to a somewhat subtle issue of principle in addressing the problem of a RAM in general, and of an R-RAM in particular. While, the case of a lossy scatterer poses no problem, that for a negative absorption (R-RAM) does raise subtle issues of the *absolute* versus the *convective* instability because of the amplification. The important difference is that a dissipative scattering system can be readily discussed (in the spirit of the linear response theory) in terms of a complex dielectric constant (or equivalently, a complex refractive index $n(\omega) = n'(\omega) + in''(\omega)$ with $n''(\omega) > 0$ for dissipation) that describes the steady-state response which is insensitive to the initial (switching) condition inasmuch as the transients die out. This is not the case for the negative absorption ($n''(\omega) < 0$) – here, one is forced to carry the transients from an initial switching condition as they grow with time and there is no steady-state! This would seem to invalidate the use of $n''(\omega) < 0$ for the R-RAM case in particular. This, however, is not the case. The crucial point to note here is the following. While, for a spatially confined homogeneous system (ideally a closed laser cavity) $n''(\omega) < 0$ will give an *absolute* temporal instability of the standing wave modes where the initial transients will grow, this is not true for a *convective* system [1]. Here, the energy is *convected away* by the propagating wave which, of course, grows in amplitude before exiting the system. The RAM is essentially such a convective open system. This is implicitly taken care of by the complex wavevector $|\omega n''(\omega)/c|$ and *not* by a complex frequency. Mathematically, the case of negative absorption ($n''(\omega) < 0$) for the physically convective system has to be viewed as an analytic continuation from the case of dissipation ($n''(\omega) > 0$) as a control parameter, e.g., pumping (or l_g) is varied. This permits, e.g., the use of Mie scattering expressions [2] for the active scatterers in our Monte Carlo studies on R-RAMs with due change of sign that turns σ_a (for absorption) into σ_{na} (for negative absorption). Based on these we present below our Monte Carlo simulations on an R-RAM [1].

[1] see Appendix C, at the end of the Thesis.

5.2 Monte Carlo simulation

Monte Carlo simulations are performed on an R-RAM (size 1 cm × 1 cm × 1 cm) consisting of passive bulk in which sub-micron sized active scatterers are randomly embedded. In the simulation, a seed photon is assumed to be spontaneously emitted (or injected) at some position (x, y, z) lying within the sample volume. The position coordinates are picked randomly from a uniform distribution. This seed photon travels along some random direction for a distance l, where, it encounters a scattering event which changes its direction of propagation probabilistically. Photon's free path length is taken to be distributed exponentially. It was simulated through $l_i = -l_s\ ln\ (random)$, where, l_i is the distance traversed between the i^{th} and the $(i+1)^{th}$ consecutive scattering events, $l_s = 1/n_s\sigma_s$ is the scattering mean free path and *random* is a uniform variate in the interval (0,1). Here, n_s is the scatterer density, and σ_s is the scattering cross-section of the active scatterer (calculated using the BHMIE subroutine in [2]). It is important to note that "σ_s" is governed by both the real and the imaginary (negative in our case of amplifying scatterers) parts of the refractive index of the active scatterer. The direction of the scattered photon (θ) is taken to be given by the Henyey-Greenstein probability distribution function [3]:

$$P(\theta) = \frac{1 - g^2}{(1 + g^2 - 2gcos\theta)^{3/2}} \tag{5.1}$$

that accounts for the anisotropy in scattering. Here, $g =< cos\theta >$ is the anisotropy parameter (calculated using the BHMIE subroutine in [2]). The azimuthal angle ϕ is chosen from a uniform distribution over the interval $(0,2\pi)$.

The path of the photon is thus monitored keeping track of its position (x, y, z) coordinates, the directions of propagation (scattering angles θ, ϕ) and the total number of scattering events (N_{scat}) it undergoes before finally exiting the R-RAM, that is, when at least one of its position coordinates exceeds the sample volume. At each event of scattering on an active scatterer, the photon is multiplicatively amplified by a factor σ_{total}/σ_s, giving the total amplification factor $(\sigma_{total}/\sigma_s)^{N_{scat}}$ for this tracked photon. Here, σ_{total} $(= \sigma_s + \sigma_{na})$ is inclusive of the negative absorption by the scatterer (as defined below). Equivalently, the corresponding amplified

intensity (I) is given by

$$I = I_o(\sigma_{total}/\sigma_s)^{Nscat} = I_o exp\,[N_{scat}\ ln((\sigma_s + \sigma_{na})/\sigma_s)]\ , \tag{5.2}$$

Here, σ_s is the scattering cross-section that governs the mean free path l_s (as discussed above). On the other hand, the cross-section σ_{na} is a measure of the photon gain induced by an active scatterer due to its negative absorption (hence the subscript 'na' in σ_{na}), or gain. In the Mie-theoretical calculation (BHMIE subroutine in [2]), σ_{na} is obtained as the usual absorption cross-section (σ_a) but with the sign reversed corresponding to change of sign of the imaginary part of the refractive index (which is positive for absorption/loss and negative for amplification/gain). The use of the Mie expression for the scattering cross-section, as the imaginary part changes sign from dissipation to negative absorption, is justified from our discussion in the Introduction.

As the photon may exit from any face, the calculated intensity constitutes the total emission intensity from all faces. This process (simulation run) of tracing the path of a spontaneously emitted photon within the R-RAM till it exits is repeated $N \sim 500{,}000$ times, each run effectively corresponding to a different realization of the R-RAM. The mean intensity is obtained by summing up the intensities obtained in the various simulation runs and dividing the sum by the total number of such runs (photon paths).

Here, we would like to emphasize the distinction in the way, the random walk of a photon in a D-RAM (chapter 3) and that in an R-RAM is simulated. In a D-RAM, we track the trajectory of the spontaneously emitted seed photon that undergoes scattering off the passive scatterers and amplification within the active bulk medium, till it finally exits the D-RAM. Thus, the parameter of interest which gives the resulting light amplification, is the total path length of the photon in the bulk (active) medium. On the other hand, in an R-RAM, as we track the path of the spontaneously emitted photon undergoing scattering events into the passive bulk medium and amplification within the interior of the active scatterer, the parameters that control the resulting light amplification are the number of scattering events (N_{scat}), the scattering (σ_s) and the gain (σ_{na}) cross-sections; *not* the path length of the photon through the bulk (passive).

Samples with active scatterer sizes 0.04 μm – 0.14 μm, embedded in the passive bulk

medium were considered. The emission wavelength (λ) within the active medium (scatterer) was taken to be 0.80 μm. Clearly, the scatterer sizes are in the sub-wavelength regime ruling out geometrical optics. The gain length (l_g) was varied over a wide range from 0.04 μm (high gain) to 0.20 μm (low gain). Since the scatterers are active, their refractive index is taken to be a complex quantity ($n'_{sphere} - in''_{sphere} : n''_{sphere} > 0$). While the real part of the scatterer's refractive index (n'_{sphere}) was kept fixed at 2.3, the imaginary part (n''_{sphere}) was calculated from the gain length ($n''_{sphere} = \lambda/4\pi l_g$). The refractive index of the passive bulk (n_{bulk}, which is real) was varied from 1.5 to 2.28 (in steps of 0.01). Thus, for a given set of parameters characterizing the R-RAM (e.g. λ, n''_{sphere}, l_g, d), the refractive index mismatch ($\Delta n = n'_{sphere} - n_{bulk}$), in the real part of the refractive indices of the active scatterers and the passive bulk, was varied from 0.02 to 0.8. The active scatterer densities were varied from 6 $\times 10^{11}$/cc to 3×10^{15}/cc which ensured that the photon undergoes sufficient scattering events before it finally exits the R-RAM and still the particle size is less than the mean particle spacing.

5.3 Results

Before proceeding to our Monte Carlo simulation for multiple scattering in an R-RAM, we give, for the sake of completeness, the results for the various cross-sections (σ_s and σ_{na}), for a single active scatterer. These have been calculated using the standard Mie theory (BHMIE subroutine in [2]). Figures 5.2 and 5.3 give the scattering and the negative absorption/gain cross-sections as function of refractive index mismatch (Δn) for different gain lengths, for a single active scatterer of size 0.04 μm and 0.14 μm respectively.

Now, we turn to our simulation results for a collection of active scatterers in an R-RAM (the results calculated above for the single active scatterer are now inputs to the case of multiple scattering.

We first consider the case for low gain (large l_g). Figure 5.4(a) shows the mean of logarithm of emission intensity ($< lnI >$) as function of the refractive index mismatch (Δn) with scatterer (active) size = 0.04 μm, scatterer density = 3×10^{15}/cc and gain length l_g = 0.20

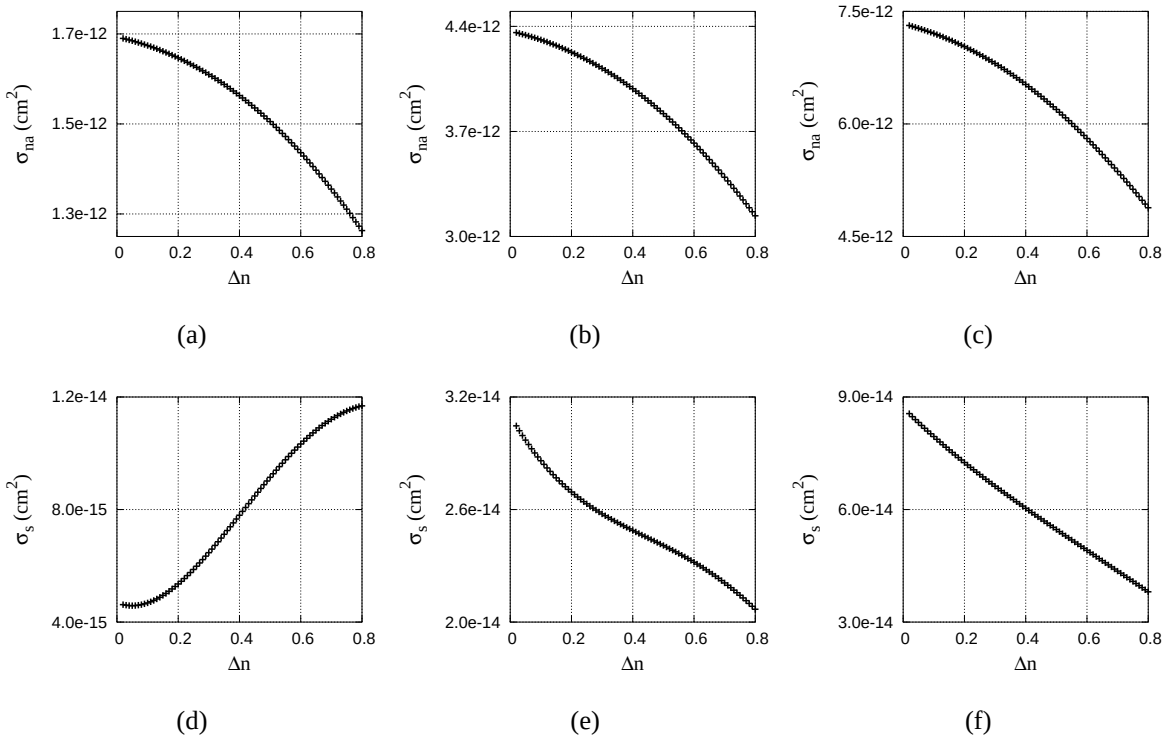

Figure 5.2: *Negative absorption cross-section (σ_{na}) as function of refractive index mismatch (in the real parts) for scatterer size = 0.04 μm with (a) l_g = 0.20 μm, (b) l_g = 0.08 μm, (c) l_g = 0.05 μm; Scattering cross-section (σ_s) as function of refractive index mismatch (in the real parts) for (d) l_g = 0.20 μm (e) l_g = 0.08 μm (f) l_g = 0.05 μm.*

μm (low gain). We would like to point out that each point (mean intensity value) on the curve is an average over 500,000 simulation runs (photon paths). It is evident from figure 5.4(a) that $< lnI >$ increases monotonically with the increase in Δn. This emission feature is similar to that observed for a D-RAM, where the mean emission intensity increases over the entire range of refractive index mismatch. This can be interpreted as follows : As in the case of D-RAM, increase in Δn enhances the multiple scattering in the R-RAM too, leading to enhanced amplification. In the case of R-RAM, however, there is an additional effect to be considered, namely, that the increase in refractive mismatch leads to a decrease in the penetration of photon into the interior of the active scatterer. In the case of low-gain R-RAM, the latter is not a dominant effect.

Now, we discuss the case of high gain (small l_g). Figure 5.4(c) gives $< lnI >$ as function

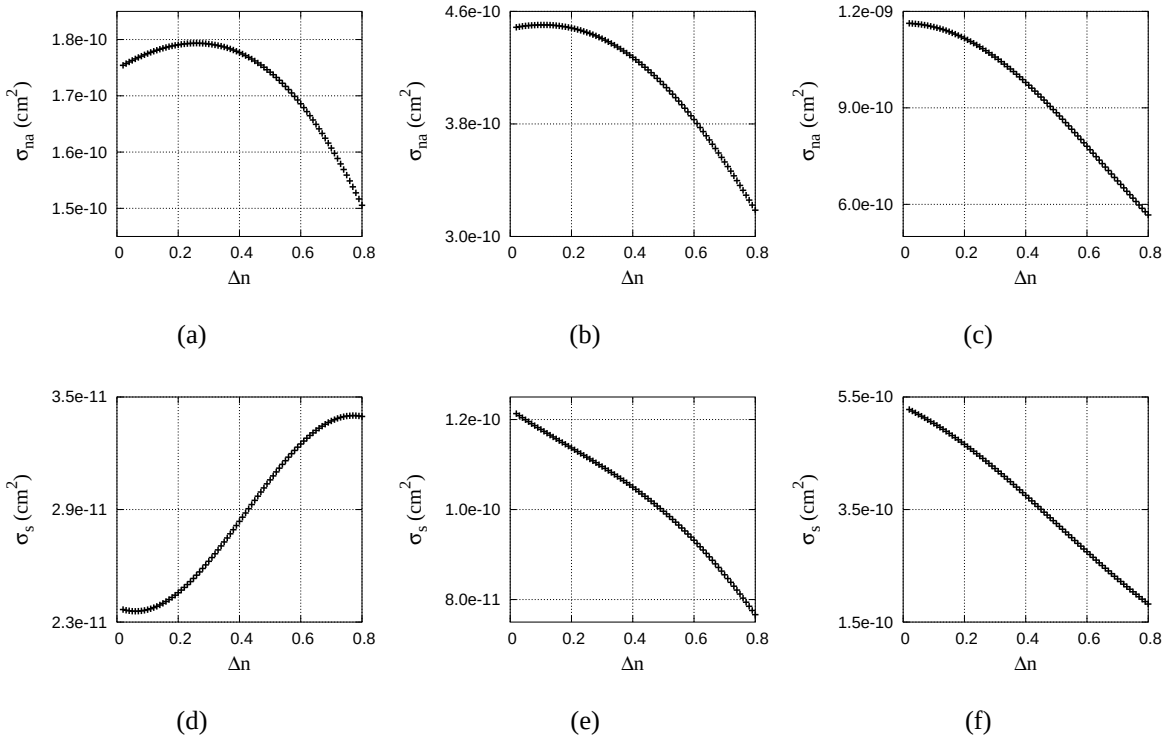

Figure 5.3: *Negative absorption cross-section (σ_{na}) as function of refractive index mismatch (in the real parts) for scatterer size = 0.14 μm with (a) l_g = 0.11 μm, (b) l_g = 0.06 μm, (c) l_g = 0.04 μm; Scattering cross-section (σ_s) as function of refractive index mismatch (in the real parts) for (d) l_g = 0.11 μm (e) l_g = 0.06 μm (f) l_g = 0.04 μm.*

of Δn for enhanced gain or decreased gain length (l_g = 0.05 μm). Here, the mean intensity decreases monotonically with increase in Δn. This indicates that the scattering within the R-RAM is too strong and, therefore, effectively reduces the photon penetration into the interior of the active scatterer and thus suppresses its amplification. This effect (unfavourable to amplification) now dominates over the increase in frequency of encountering the active scatterers (favourable to amplification). In fact, the photons are repeatedly scattered back into the passive bulk, where they are not amplified.

Figure 5.4(b) gives $< lnI >$ as function of Δn for the intermediate gain length (l_g = 0.08 μm). This corresponds to the crossover regime.

Now, we examine the effect of increasing the scatterer (active) size on the emission features. Figures 5.5(a-c) show the variation of $< lnI >$ as function of refractive mismatch (Δn),

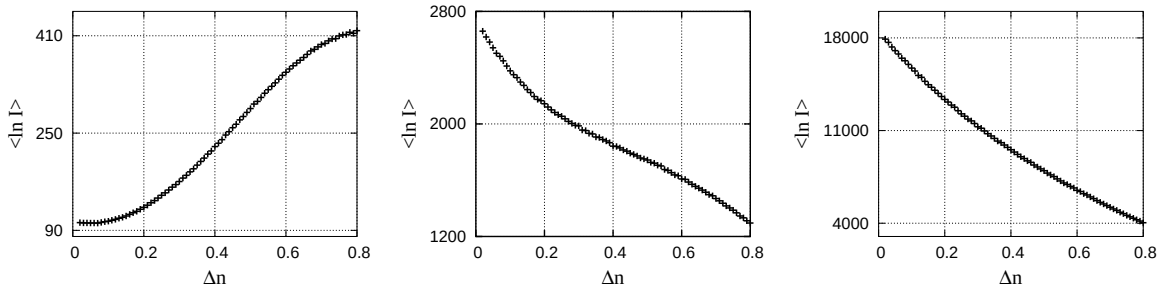

(a) (b) (c)

Figure 5.4: *Mean intensity as function of refractive index mismatch (in the real parts) for scatterer size = 0.04 μm, density = 3 $\times 10^{15}$/cc with (a) l_g = 0.20 μm, (b) l_g = 0.08 μm, (c) l_g = 0.05 μm.*

for scatterer size of 0.14 μm, density = 6×10^{11}/cc at l_g of 0.11 μm, 0.06 μm, and 0.04 μm, respectively. As the higher scatterer (active) size favours light amplification, the monotonic increase in mean intensity with Δn is observed even for l_g as small as 0.11 μm (less than the size of the active scatterer). In fact, much higher gains (or lower gain lengths) are required to observe a decrease in mean intensity with the corresponding increase in Δn.

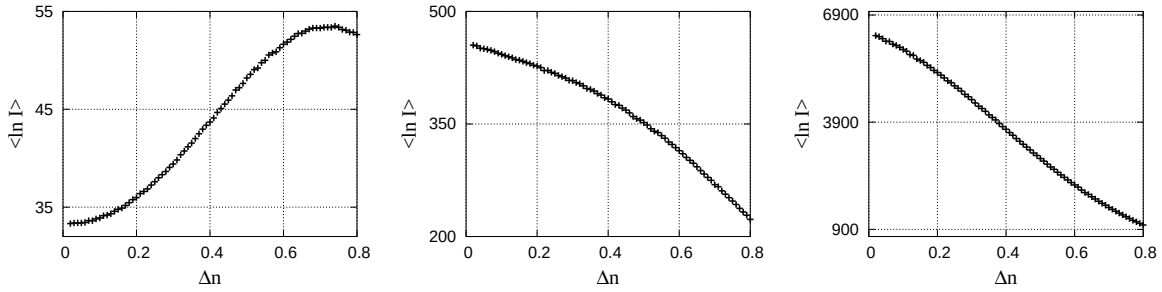

(a) (b) (c)

Figure 5.5: *Mean intensity as function of refractive index mismatch (in the real parts) for scatterer size = 0.14 μm, density = 6×10^{11}/cc with (a) l_g = 0.11 μm, (b) l_g = 0.06 μm, (c) l_g = 0.04 μm.*

5.4 Conclusions

We have performed a detailed study, via Monte Carlo simulations, of the emission intensity from an R-RAM as function of refractive index mismatch (Δn) in the real part of the refractive indices of the active scatterers and the passive bulk, for a wide range of parameters characterizing the R-RAM. The simulation results quite clearly show the marked difference in the emission features of an R-RAM from that of a D-RAM. In particular, for a D-RAM (characterized by certain gain (l_g^{-1})), the larger the scattering strength (controlled by scatterer density, scatterer size or refractive index mismatch in the active bulk and the passive scatterers), the larger is the diffusive path-length or dwell time of photons in the active bulk. This always results in the enhanced light amplification. Contrary to this, very large scattering strength (controlled by refractive index mismatch) within an R-RAM is detrimental to the light amplification as larger scattering off the active scatterers in an R-RAM serve to scatter the photons back to the passive bulk thereby not allowing them to penetrate the interior of the active scatterer. This, thus, leads to the observed drop in light amplification in an R-RAM, at large scattering strengths. However, in order to bring out this feature very clearly in our simulation, we have made a choice for the value of the gain length l_g which is very small corresponding to very high gain.

It is worth pointing out that, since in an R-RAM, the active particles perform the dual role of light amplification and light scattering, the observed net amplification depends on the relative strength of the two opposing effects, namely, the frequency of visits to the active scatterers and the effectiveness of visiting the interior of the active scatterer.

Finally, it is to be emphasized that the scattering and the amplification by an individual active scatterer are affected qualitatively differently by the parameters of the active scatterer. This point can be appreciated clearly by considering an elementary example of an active scatterer in the form of a slab geometry for a normally incident beam (see Appendix D, at the end of the Thesis).

Bibliography

[1] D.B. Melrose and R.C. McPhedran, *Electromagnetic processes in dispersive media*, Cambridge University Press, Cambridge, 1991.

[2] C.F. Bohren and D.R. Huffman, *Absorption and Scattering of light by small particles*, (Wiley, New York, 1983).

[3] L.C. Henyey and J.L. Greenstein, Astrophys. J. 93 (1941) 70.